ELSEVIER

Journal of Process Control 9 (1999) 375–383

JOURNAL OF PROCESS CONTROL

Globally optimal robust process control

Jeremy G. VanAntwerp, Richard D. Braatz*, Nikolaos V. Sahinidis

University of Illinois at Urbana-Champaign, Department of Chemical Engineering, 600 South Mathews Avenue, Box C-3, Urbana, IL 61801-3792, USA

Abstract

A computational approach is developed for designing a globally optimal controller which is robust to time-varying nonlinear perturbations in the plant. This controller design problem is formulated as an optimization with bilinear matrix inequality (BMI) constraints, and is solved to optimality by a branch and bound algorithm. The algorithm is applied to a reactive ion etcher, and provides superior performance while providing robustness to nonlinear plant/model mismatch. The algorithm is also applied to a well known benchmark problem.

Keywords: Robust control; Time-varying nonlinear perturbations; Optimal control of uncertain systems

1. Introduction

In practice, *any* model is an inaccurate representation of the true process. Robust control addresses this plant/model mismatch by defining a set of plants of which the true process is an element. This set is defined by an uncertainty description. Controllers are designed to be robust to the uncertainty, that is, to achieve a desired level of performance for any plant in the set.

The most popular method for designing robust controllers is DK-iteration, which involves alternately solving for the controller K and the appropriate scaling matrix D. Since DK-iteration is an ad hoc approach applied to a nonconvex problem, the resulting controller can be suboptimal. In spite of the fact that DK-iteration is not guaranteed to converge to a global optimum, it has been applied to a large number of academic case studies such as high purity distillation columns, CSTRs, and packed bed reactors [1,2]. However, recent examples have illustrated that DK-iteration can provide conservative controller designs, even for processes of relatively small dimension [3].

Having a conservative controller is undesirable, especially since the cost of obtaining an uncertainty description can be high. Algorithms to compute a globally optimal robust controller have been proposed [4,5]. The formulation of Goh et al. [4] requires iterative solutions of nonconvex feasibility problems, each of which is solved via branch and bound. Yamada et al. [5] solve the optimization problem directly but the computational requirements of their proposed algorithm grows rapidly as a function of the number of uncertainties. Here an approach is developed for computing a globally optimal controller which is robust to time-varying nonlinear perturbations in the plant. The controller design problem is directly formulated as an optimization with bilinear matrix inequality (BMI) constraints. A branch and bound technique is then used to find a global solution. The proposed algorithm provides tighter bounds, and a more direct numerical approach, than previous algorithms.

The next sections provide background on linear and bilinear matrix inequalities (LMIs and BMIs), robust control, and the branch and bound global optimization approach. Then we present LMI upper and lower bounds for the BMI problem that are used in a branch and bound algorithm to compute a globally optimal robust controller. Lastly, the algorithm is applied to an industrially relevant microelectronics process. To the authors' knowledge, the corresponding optimization problem is the largest BMI control problem ever solved.

2. LMIS and BMIS

A Linear Matrix Inequality (LMI) has the form [6]:

$$F(x) = F_0 + \sum_{i=1}^{m} x_i F_i \geqslant 0 \tag{1}$$

* Corresponding author. Tel: +1-217-333-5073; fax: +1-217-333-5052; e-mail:braatz@uiuc.edu

0959-1524/99/$ - see front matter
PII: S0959-1524(99)00012-8

where $x \in \mathcal{R}^m$, $F_i \in \mathcal{R}^{n\times n}$, $\mathcal{R}^m$ is the set of all real vectors of length m, and $R^{n\times n}$ is the set of all real $n \times n$ matrices. The symmetric matrices $F_i = F_i^T$, $i = 0, 1, \ldots, m$ are fixed and x is the variable. Thus, the symmetric matrix $F(x)$ is an affine function of the elements of x and is a positive semidefinite matrix, that is $z^T F(x) z \geqslant 0$, $\forall z \neq 0, z \in \mathcal{R}^n$. The LMI [Eq. (1)] is equivalent to n polynomial inequalities because a matrix is positive semidefinite if and only if each leading principal minor of $F(x)$ is nonnegative. An important property of LMIs is that the set $\{x|F(x) \geqslant 0\}$ is convex, that is, the LMI [Eq. (1)] forms a convex constraint on x.

The form of an LMI is very general; linear inequalities, (convex) quadratic inequalities, matrix norm inequalities, and various constraints from control theory such as Lyapunov and Riccati inequalities can all be written as LMIs. Moreover, multiple LMIs can always be written as a single LMI of larger dimension. LMIs form convex sets, and optimization problems with LMI constraints are solvable in polynomial-time with off-the-shelf software [7,8].

A bilinear matrix inequality (BMI) is of the form:

$$F(x, y) = F_0 + \sum_{i=1}^{m} x_i F_i + \sum_{j=1}^{k} y_j G_j + \sum_{i=1}^{m}\sum_{j=1}^{k} x_i y_j H_{ij} \geqslant 0 \tag{2}$$

where G_j and H_{ij} are symmetric matrices of the same dimension as F_i, and $y \in \mathcal{R}^k$.

The bilinear terms make the set $\{x, y \mid F(x, y) \geqslant 0\}$ nonconvex and no off-the-shelf software exists for solving optimization problems with BMI constraints. It is straightforward to prove that BMI optimization problems are NP-hard, which implies that it is highly unlikely that there exists a polynomial-time algorithm for solving these problems. The control problems considered in this paper are a special form of Eq. (2):

$$F(x) = F_0 + \sum_{i=1}^{m} x_i F_i + \sum_{j=1}^{m} y_j G_j \geqslant 0 \qquad x_i y_i \leqslant 1 \quad \forall i \tag{3}$$

although the results hold for the general form as well [see Eqs. (15–18)].

3. Robustness

Any process model is only an approximation of the true process. In robust control, the true plant P_{true} is covered by a set of plants $\hat{P}$ which is represented by the nominal model P and a set of norm bounded perturbations χ_Δ^t.

$$\hat{P} = f(P, \chi_\Delta^t) \tag{4}$$

$$P_{\text{true}} \in \hat{P}$$

For robust controller synthesis, the finite-dimensional linear time-invariant controller K is designed to stabilize all plants within the set (e.g. see Fig. 1). The block diagram of the uncertain closed loop system is rearranged to give either of the *equivalent* block diagrams of Fig. 2. The purpose is to collect the uncertainties into a single block diagonal matrix Δ where each block represents an uncertainty associated with either a parameter or component of the process (e.g. unmodeled dynamics or nonlinearity). The nominal plant P, which corresponds to $\Delta = 0$, is finite-dimensional linear time-invariant. The generalized plant matrix G is determined from the nominal plant P by the performance and uncertainty weights (e.g. see Fig. 8), and the location and structure of the uncertainties. The closed loop transfer function matrix $M(K)$ is a linear fractional transformation (LFT) of G and K [1,2]. The plant input w contains the desired set point, measurement noise, and disturbances. The output z contains the variables to be controlled.

The set of proper (realizable) controllers that internally stabilize G is denoted by $\mathcal{K}_s$. The set χ_Δ is the set of block diagonal matrices $\{\text{diag}\{\Delta_k\} | \Delta_k \in C^{r_k\times r_k}, \sum_k r_k = n\}$, where $C^{r_k\times r_k}$ is the set of all $r_k \times r_k$ matrices with complex entries. The set χ_Δ^t is the set of all time-varying operators $\Delta(t)$ with the same block diagonal structure as χ_Δ and bounded such that $\bar{\sigma}(\Delta(t)) \leqslant 1$, $\forall t \geqslant 0$.

For a fixed $\Delta \in \chi_\Delta^t$ and a controller $K \in \mathcal{K}_s$ let $T_{zw}(K, \Delta)$ denote the closed loop mapping from w to z. The objective of robust controller design is to solve

$$\gamma^* = \inf_{K\in\mathcal{K}_s} \sup_{\Delta\in\chi_\Delta^t} \| T_{zw}(K, \Delta) \|. \tag{5}$$

where $\|\cdot\|$ is the operator 2-norm. The performance specification is satisfied for all plants within the uncertainty description if and only if $\gamma^* < 1$. The optimization in Eq. (5) is neither concave nor convex and is difficult to solve. For nonlinear time-varying uncertainty, Eq. (5) is equivalent to [3]:

$$\gamma^* = \inf_{K\in\mathcal{K}_s} \inf_{\substack{D\in\mathcal{D}\\ \gamma>0}} \gamma \tag{6}$$

such that

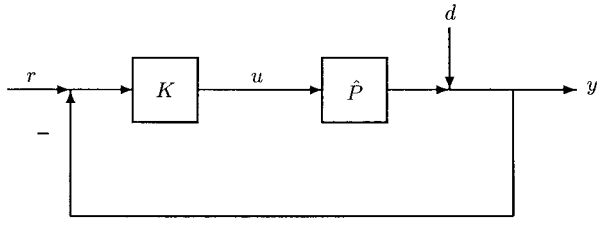

Fig. 1. Closed loop uncertain system.

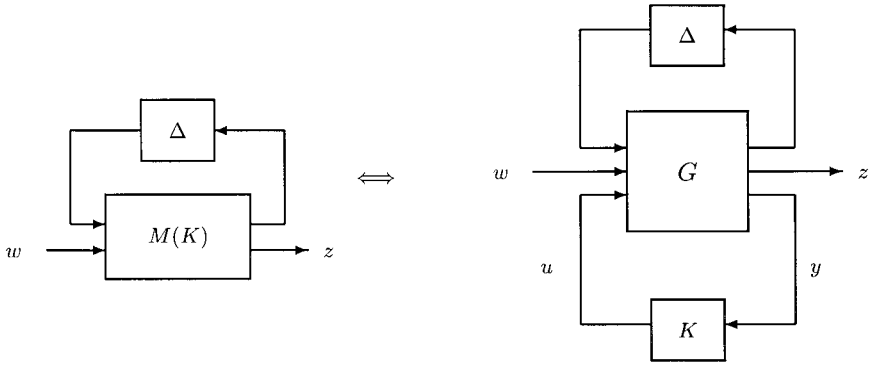

Fig. 2. Equivalent uncertain systems.

$$\left\| \begin{bmatrix} D & 0 \\ 0 & \gamma I \end{bmatrix}^{-1/2} M(K) \begin{bmatrix} D & 0 \\ 0 & \gamma I \end{bmatrix}^{1/2} \right\|_{\infty} < 1. \tag{7}$$

where $\mathcal{D}$ is the set of structured scaling matrices $\mathcal{D} \equiv \{\mathrm{diag}\{d_k I_{r_k}\} \mid 0 < d_k \in \mathcal{R}, \sum_k r_k = n\}$, $\mathcal{R}$ is the set of real numbers, and I is the identity matrix of appropriate dimension.

That the optimization over $\Delta \in \chi_{\Delta}^{t}$ can be replaced by an optimization over $D \in \mathcal{D}$ is a well known result shown by Shamma [9,10]. The optimization over $D \in \mathcal{D}$ is also a nonconvex optimization, but one for which a sub-optimal solution can be computed by a technique known as DK-iteration. It is possible to formulate the constrained optimization [Eqs. (6) and (7)] as a problem which is convex in one set of variables (associated with D) and is convex in another set of variables (associated with K), but there is no known formulation which is jointly convex in all of the variables. DK-iteration solves for K with a fixed D and then solves for D with a fixed K, alternating until the objective function is no longer decreased. Although DK-iteration is not guaranteed to converge to a global optimum, it has been applied to a large number of academic case studies such as high purity distillation columns, CSTRs, and packed bed reactors [1,2]. It should be further noted that when D is allowed to be a function of frequency rather than constant, Eqs. (6) and (7) form a commonly used upper bound for the case of linear time-invariant uncertainty Δ.

Let the state space realization for the generalized plant $G(s) = C(sI - A)^{-1}B + D$ be represented by

$$G = \left[\begin{array}{c|cc} A & B_1 & B_2 \\ \hline C_1 & D_{11} & D_{12} \\ C_2 & D_{21} & D_{22} \end{array}\right], \tag{8}$$

where $D_{22} = 0$ without loss of generality [11]. Then Eqs. (6) and (7) maybe written as an optimization with BMI constraints:

$$\gamma^* = \inf_{\substack{(L,R,X,Y)\in\mathcal{B} \\ \rho(L_1 R_1)\leqslant 1}} \gamma \tag{9}$$

where ρ is the spectral radius and $\mathcal{B}$ is the set such that L, R, X and Y are symmetric matrices,

$$L = \begin{bmatrix} L_1 & 0 \\ 0 & \gamma I \end{bmatrix}; R = \begin{bmatrix} R_1 & 0 \\ 0 & \gamma I \end{bmatrix}; L_1, R_1 \in \mathcal{D}; \tag{10}$$

and

$$Q_1 \begin{bmatrix} AX + XA^T & XC_1^T & B_1 \\ C_1 X & -L & D_{11} \\ B_1^T & D_{11}^T & -R \end{bmatrix} Q_1^T < 0; \tag{11}$$

$$Q_2 \begin{bmatrix} YA + A^T Y & YB_1 & C_1^T \\ B_1^T Y & -R & D_{11} \\ C_1 & D_{11}^T & -L \end{bmatrix} Q_2^T < 0; \tag{12}$$

$$\begin{bmatrix} X & I \\ I & Y \end{bmatrix} > 0; \tag{13}$$

where

$$Q_1 = \begin{bmatrix} \begin{pmatrix} B_2 \\ D_{12} \end{pmatrix}^{\perp} & 0 \\ 0 & I \end{bmatrix}; Q_2 = \begin{bmatrix} \begin{pmatrix} C_2^T \\ D_{21}^T \end{pmatrix}^{\perp} & 0 \\ 0 & I \end{bmatrix}. \tag{14}$$

Here $A^{\perp}$ is a matrix whose rows form the basis for the null space of A^T. The optimization in Eq. (9) is nonconvex because of the spectral radius constraint.

In this paper, LMI upper and lower bounds are derived that make Eqs. (9)–(13) well suited for the application of a branch and bound algorithm. Once Eqs. (9)–(13) has been solved (to within a desired tolerance), a globally optimal robust controller is calculated from Eqs. (6) and (7) by substituting L for D and by setting γ equal to the γ^* calculated in Eq. (9).

4. Branch and bound

A detailed description of the branch and bound algorithm is provided elsewhere [12]. However, the basic idea is as follows. First, a valid relaxation $\tilde{P}$ of a nonconvex

problem P [see Fig. 3(a)] must be obtained. In order for the relaxation to be valid, the difference between the optimal objective function values of P and $\tilde{P}$ must be a non-increasing function of the size of the feasible region over which the relaxation is obtained. Additionally, a global solution must be attainable for every relaxation (usually this means that $\tilde{P}$ should be convex). The relaxed problem is solved, providing a lower bound L for the optimal solution. Using this solution as a starting point a local minimization is performed. This yields an upper bound U on the global solution. If L is sufficiently close to U then the algorithm terminates. If not, then the domain is subdivided and the procedure is repeated for each section [see Fig. 3(b)]. If the lower bound for a region is greater than the current upper bound then that region may be discarded [see Fig. 3(c)]. Provided that at each iteration the region with the lowest lower bound is selected for processing, convergence is guaranteed, as eventually the upper and lower bounds will be equal to within the specified tolerance [see Fig. 3(d)] [13].

5. Upper and lower bounds

The art to developing an efficient branch and bound algorithm is to derive tight upper and lower bounds from the objective function over any given part of the domain. Reducing the ranges of all problem variable as much as possible is frequently a key to tight objective function bounding. A lower bound to the performance problem Eqs. (9)–(13) is

$$\inf_{\substack{(L,R,X,Y)\in\mathcal{B}\\ \underline{l}_i\leqslant l_i\leqslant\bar{l}_i\\ \underline{r}_j\leqslant r_j\leqslant\bar{r}_j\\ F_0+\sum_i\sum_j l_i r_j F_{ij}\geqslant 0}} \gamma \geqslant \inf_{\substack{(L,R,X,Y)\in\mathcal{B}\\ \underline{l}_i\leqslant l_i\leqslant\bar{l}_i\\ \underline{r}_i\leqslant r_i\leqslant\bar{r}_i\\ F_0+\sum_i\sum_j w_{ij}F_{ij}\geqslant 0\\ w_{ij}\in[\underline{w}_{ij},\bar{w}_{ij}]}} \gamma \tag{15}$$

where the overbar (underbar) indicates the upper (lower) bound for a variable and

$$\underline{w}_j = \min\left\{\underline{l}_i\underline{r}_j, \bar{l}_i\underline{r}_j, \underline{l}_i\bar{r}_j, \bar{l}_i\bar{r}_j\right\} \tag{16}$$

$$\bar{w}_{ij} = \max\left\{\underline{l}_i\underline{r}_j, \bar{l}_i\underline{r}_j, \underline{l}_i\bar{r}_j, \bar{l}_i\bar{r}_j\right\} \tag{17}$$

Further, because w_{ij} is a bilinear term the following additional constraints may be included in the lower bound [Eq. (15)] [14].

$$\begin{aligned} w_{ij} &\leqslant \underline{r}_j l_i + \bar{l}_i r_j - \underline{r}_j\bar{l}_i\\ w_{ij} &\leqslant \underline{l}_i r_j + \bar{r}_j l_i - \underline{l}_i\bar{r}_j\\ w_{ij} &\geqslant \bar{l}_i r_j + \bar{r}_j l_i - \bar{r}_j\bar{l}_i\\ w_{ij} &\geqslant \underline{l}_i r_j + \underline{r}_j l_i - \underline{l}_i\underline{r}_j \end{aligned} \tag{18}$$

An LMI upper bound is obtained by fixing some of the variables:

$$\inf_{\substack{(L,R,X,Y)\in\mathcal{B}\\ \underline{l}_i\leqslant l_i\leqslant\bar{l}_i\\ \underline{r}_j\leqslant r_j\leqslant\bar{r}_j\\ \rho(l_i r_j)\leqslant 1}} \gamma \leqslant \inf_{\substack{(L,R,X,Y)\in\mathcal{B}\\ l_i=\underline{l}_i\\ \underline{r}_j\leqslant r_j\leqslant\bar{r}_j\\ \rho(l_i r_j)\leqslant 1}} \gamma \tag{19}$$

With these polynomial-time computable LMI upper and lower bounds, the nonconvex optimization Eqs. (9)–(13) is ideal for the application of the branch and bound algorithm.

Upper and lower bounds for each of the variables (the under- and overlined variables in the above equations) may be computed by solving an LMI of dimension similar to Eqs. (9)–(13) [15].

6. Mass–spring benchmark problem

Consider a mechanical system of two masses connected by a spring (see Fig. 4) [3,16]. This extensively studied benchmark is a simple control problem formulated to capture many of the features of more complex aircraft and space structure control problems. It has been included here in order to compare the accuracy of the BMI/branch and bound technique with the accuracy of DK and LR-iteration (a variant of DK-iteration, see [3]). It is desired to control the positions of the two masses. There is one actuator (on mass 1) and one sensor (on mass 2), i.e. the sensor and actuator are noncollocated. This makes the system much more difficult to control than in the collocated case. It is assumed that the system has negligible damping. All of the parameters of the system are known with certainty except for mass 2. In state space form the system is represented as [3]:

$$\dot{x} = \begin{bmatrix}\dot{x}_1\\ \dot{x}_2\\ \dot{x}_3\\ \dot{x}_4\end{bmatrix} = \begin{bmatrix}0 & 0 & 1 & 0\\ 0 & 0 & 0 & 1\\ -k/m_1 & k/m_1 & 0 & 0\\ k/m_2 & -k/m_2 & 0 & 0\end{bmatrix}\begin{bmatrix}x_1\\ x_2\\ x_3\\ x_4\end{bmatrix} + \begin{bmatrix}0\\ 0\\ 1/m_1\\ 0\end{bmatrix}(u+0.1d) \tag{20}$$

$$y = x_2 + 0.1v \tag{21}$$

where m_1 and m_2 are the masses and k is the spring constant. The positions of the two masses are x_1 and x_2

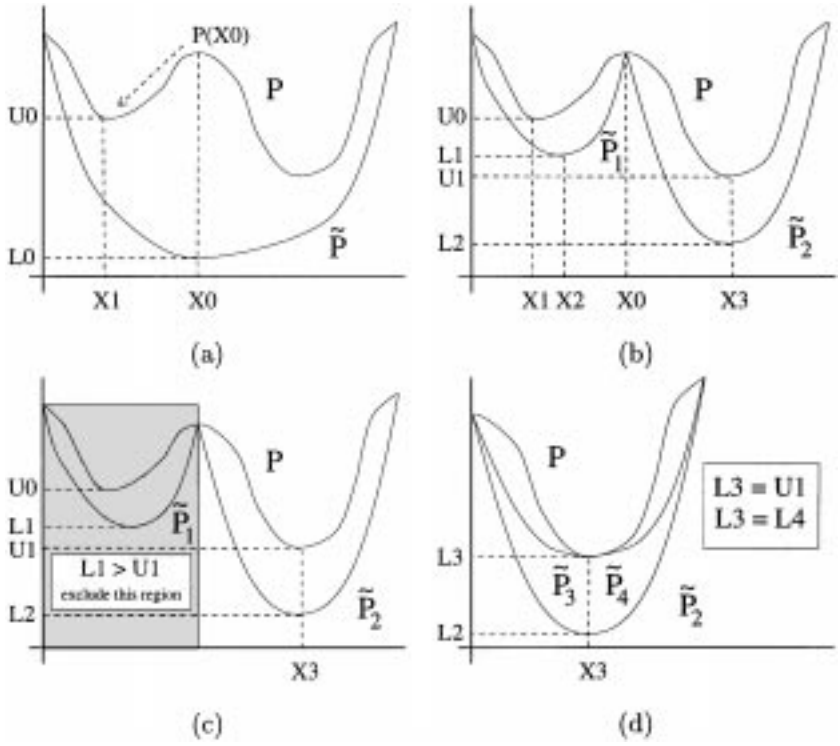

Fig. 3. The branch and bound algorithm.

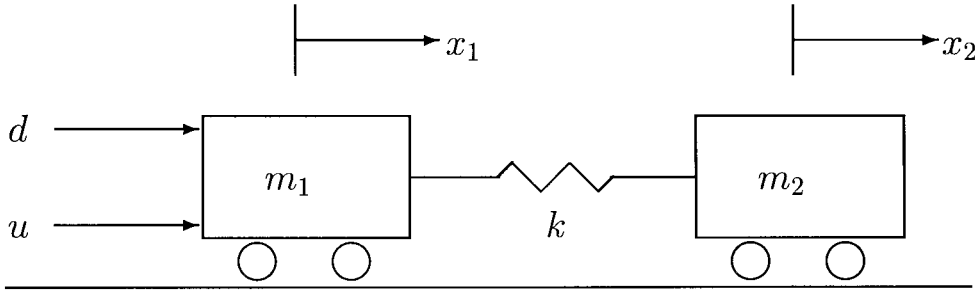

Fig. 4. Mass-spring system.

with velocities x_3 and x_4 respectively. The control input is u and the process and measurement noises are d and v.

For $m_1 = k = 1$ and $m_2 = 0.5 + w_{m_2}\delta$ this gives the generalized plant (see Fig. 2) [3]

$$G = \left[\begin{array}{cccc|cccc} 0 & 0 & 1 & 0 & 0 & 0 & 0 & 0 \\ 0 & 0 & 0 & 1 & 0 & 0 & 0 & 0 \\ -1 & 1 & 0 & 0 & 0 & 0.1 & 0 & 1 \\ 2 & -2 & 0 & 0 & -2w_{m_2} & 0 & 0 & 0 \\ \hline 2 & -2 & 0 & 0 & -2w_{m_2} & 0 & 0 & 0 \\ 0 & 1 & 0 & 0 & 0 & 0 & 0 & 0 \\ 0 & 0 & 0 & 0 & 0 & 0 & 0 & 1 \\ \hline 0 & 1 & 0 & 0 & 0 & 0 & 0.1 & 0 \end{array}\right] \tag{22}$$

where

$$w = [d\ v]^T\ z = [x_2\ u]^T \tag{23}$$

and w_{m_2} is the weight for the uncertainty block associated with m_2 and $\delta(t) \in [-1, 1]$, $\forall t \geqslant 0$.

The global optimization algorithm presented earlier was used to design a controller for this system for varying levels of uncertainty. Fig. 5 plots the closed loop performance for the system versus the inverse of the uncertainty weight w_{m_2}. For this mass spring system the resulting controller was approximately 50% less conservative than the best controller computed with other standard techniques such as DK- and LR-iteration. The controller was of order 4.

We would like to point out that the iterative methods do not always perform so poorly. For a large scale adhesive coater, the globally optimal controller was approximately 10% less conservative than controllers designed via DK-iteration [17].

7. Reactive ion etching

Fig. 6 is a diagram of a generic plasma system [18]. A radio frequency (rf) voltage source is connected in series with a capacitor to two electrodes. The electric field generated causes gas molecules in the reactor to lose outer shell electrons. These electrons interact with other molecules causing them to lose electrons or form free radicals. Thus a reactive mix of ions, electrons, and free radicals is formed. A potential difference called the self bias voltage (V_{bias}) will develop between the two electrodes due to the facts that (i) the electrons are more mobile than the ions, (ii) the electrodes have unequal surface area, and (iii) the capacitor is too large to follow the high frequency voltage source. Ions will be accelerated by this potential difference towards the sample to be etched. The bias voltage is a key parameter in determining the etch rate since it determines the incident energy of the ions.

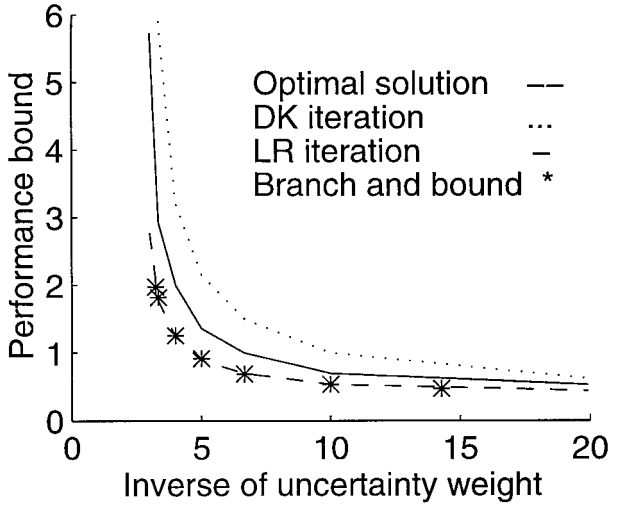

Fig. 5. Closed loop performance for mass–spring benchmark problem.

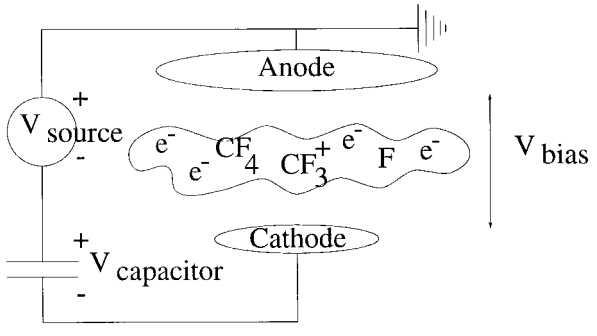

Fig. 6. Generic plasma system.

Etching is known to be a highly nonlinear, multivariable process that is strongly dependent on reactor geometry. Attempts to control etch characteristics usually manipulate the reactor pressure, gas flow rate, and the power applied to the electrodes. However, due to many disturbances, complicated reaction dynamics, and the general lack of detailed fundamental understanding of the plasma behavior, it is impossible to predict etch performance for a system given a set of inputs. In many cases, it is impossible to even predict etch performance for the same system on two different runs. For this reason, feedback control is necessary to maintain consistent etch quality. The feedback controller must be designed to be robust to the variability in process behavior as well as the nonlinear nature of the process. In the robust control approach, the uncertainty description can rigorously account for possible nonlinearities and inaccurate modeling of process dynamics.

Many of the etch parameters cannot be measured online. Instead, measurements of the plasma characteristics are made, and with these measurements the controller attempts to maintain consistent plasma characteristics. This strategy has been proven in experimental studies to give good control of the etch characteristics [19,20].

The globally optimal robust controller design procedure outlined in the previous sections was applied to the reactive ion etching (RIE) process described by Vincent et al. [20], who modeled the plasma dynamics as a static input nonlinearity N in series with a linear time-invariant (LTI) plant P_{L} (see Fig. 7). This nonlinear model was identified using an iterative least squares algorithm with data obtained from an experimental system by exciting it with a pseudo-random binary signal [20]. The identified LTI plant for their experimental RIE was

$$P_{\text{L}} = \begin{bmatrix} \frac{-1.89e^{-0.5s}(s-38.2)}{(s+5.37)(s+.160)} & \frac{-35.9(s-37.8)}{s^2+6.5s+20.2} \\ \frac{0.0239e^{-0.5s}(s-9.6)}{(s+1.05)(s+.214)} & \frac{-0.143(s-38.9)}{s^2+3.28s+4.14} \end{bmatrix} \tag{24}$$

Vincent et al. [20] selected the controller to have the form $K = \hat{N}^{-1}K_{\text{L}}$ where K_{L} is designed to stabilize the linear portion of the plant P_{L} and $\hat{N}^{-1}$ is an approximate inverse of the static nonlinearity N.

If the input nonlinearity N is identified perfectly then $\hat{N}^{-1}$ will be an exact inverse of N and there will be an identity mapping from K_{L} to P_{L}. However, if the identification is not perfect, then there will still be a nonlinear mapping from K_{L} to P_{L}. Furthermore, it is highly unlikely that the system is nonlinear only at the process input. Output nonlinearity is also a probability.

Nonlinearities in the input and output can be rigorously accounted for by the uncertainty description

shown in Fig. 8. The operators Δ_I and Δ_O can vary arbitrarily within set bounds as functions of time, and can achieve an identical input–output mapping for any possible nonlinearity within the magnitude of the bounds set by the uncertainty weights W_I and W_O.

Each uncertainty weight (W_I, W_O) was chosen to represent up to 10% steady state error and up to 100% dynamic error (in the linear case, this would be 100% error at high frequencies [1,2]). The performance weight ensures zero steady-state error and closed loop time constants of 5 and 9 s. Rearranging the block diagram in Fig. 8 results in the generalized plant matrix (see Fig. 2)

$$G = \begin{bmatrix} 0 & 0 & 0 & -W_I \\ W_O P_L & 0 & 0 & -W_O P_L \\ W_P P_L & W_P & -W_P & -W_P P_L \\ P_L & I & -I & P_L \end{bmatrix} \tag{25}$$

where

$$W_I = W_O = \frac{0.1(15s+1)}{1.5s+1} I_2 \tag{26}$$

$$W_P = \begin{bmatrix} \frac{0.5(5s+1)}{5s+0.002} & 0 \\ 0 & \frac{0.5(9s+1)}{9s+0.002} \end{bmatrix} \tag{27}$$

$$u = [T\ P_{rf}]^T; \quad y = [V_{\text{bias}}\ C_F]^T; \tag{28}$$

$$w = d; \quad Z = W_P y \tag{29}$$

The fluorine concentration in the plasma is C_F, the throttle valve position T controls the input gas flowrate, and P_{rf} is the power of the applied rf voltage.

Given this generalized plant matrix and using a third order Padé approximation for the time delays, globally optimal controller parameters were calculated by a branch and bound algorithm using the derived upper [Eq. (19)] and lower bounds [Eq. (15)]. It should be noted that the uncertainty description easily covers any possible error introduced by the time delay approximation.

The best achievable performance $\gamma^* = 0.9834$ is achieved for $L_1 = \text{diag}(0.1329I_2, 0.2623I_2)$. Since $\gamma^* < 1$, the controller satisfies the robust performance specifications. The controller is calculated from Eqs. (6) and (7) by substituting L for D and by setting γ equal to the γ^* calculated in Eq. (9). The controller was of order 48. To the authors' knowledge, this is the largest BMI control problem ever solved [the G matrix in Eq. (25) has 48 states].

For brevity, the state space matrices of the controller are reported elsewhere [21]. We did not try to reduce the order of the controller because our goal was to design the best controller—not necessarily the best controller of a specified order. Designing a robust reduced-order controller is an even harder nonconvex optimization [22–24].

Fig. 9 is a Bode plot of the open loop transfer function $P_L K_L$, which has a bandwidth very similar to the linear quadratic controller designed by Vincent et al. [20]. This is necessary in order to not magnify measurement noise. However, the globally optimal controller responds more

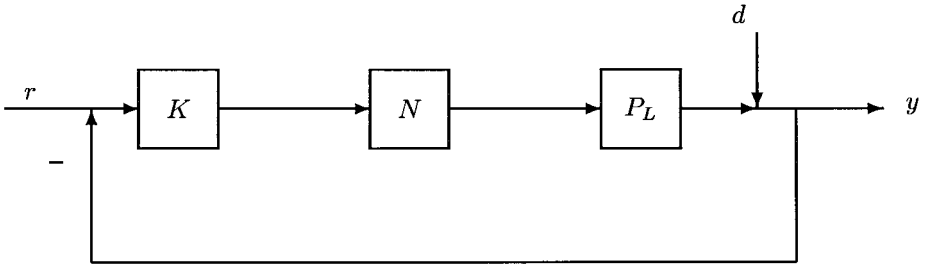

Fig. 7. RIE with input nonlinearity.

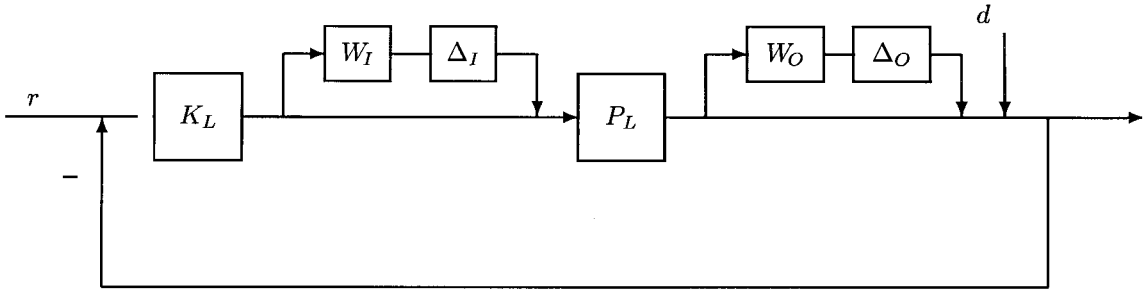

Fig. 8. RIE with input and output nonlinearities modeled as uncertainty.

than twice as fast to set point changes while at the same time providing guaranteed robustness (compare Fig. 10 with Vincent et al.'s [20] Fig. 7).

The robustness of the closed loop system to norm-bounded, nonlinear, time-varying perturbations is illustrated in Fig. 11. The time-varying operator Δ has maximum norm and instantaneously flips sign in the middle of every ramped set point change for V_{bias}. This is a difficult perturbation to suppress, yet the controller keeps the system within the performance bounds.

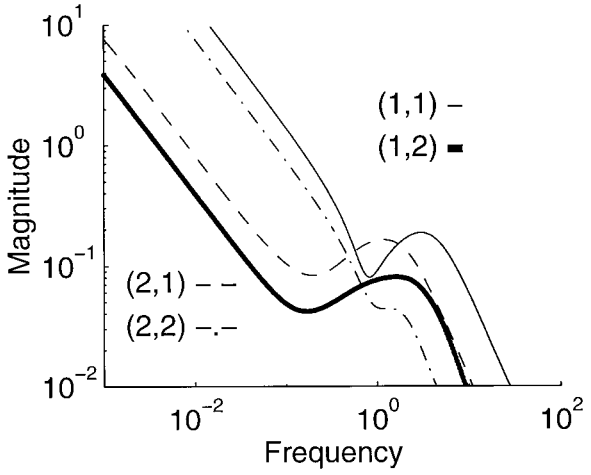

Fig. 9. Open loop Bode plot.

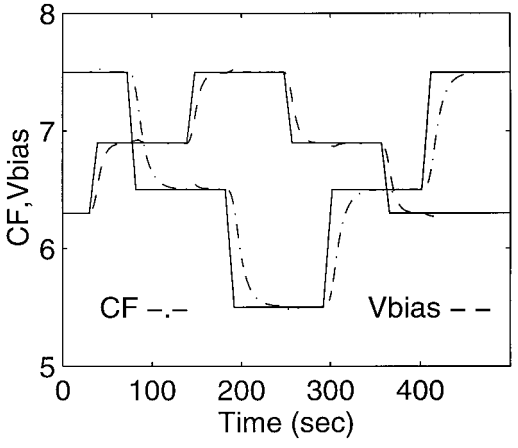

Fig. 10. Closed loop system time response.

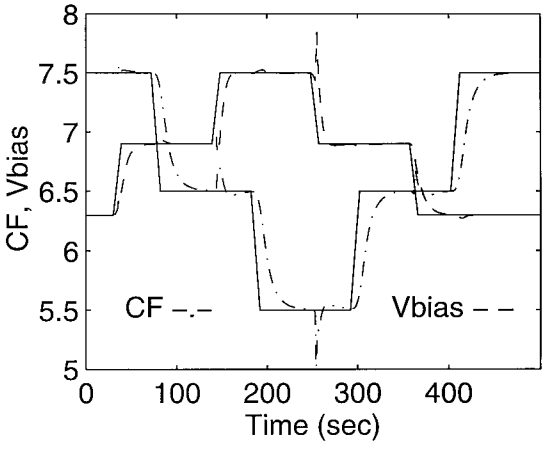

Fig. 11. Perturbed system time response.

8. Conclusions

A computational approach that directly addresses nonlinear time-varying model uncertainties in a globally optimal manner was applied to a reactive ion etcher and a mass–spring system. The resulting controller for the reactive ion etcher was robust to perturbations associated with both process inputs and outputs, while providing substantially improved dynamic response compared to a linear quadratic controller. For the mass–spring benchmark problem, the resulting controller was 50% less conservative than controllers designed via DK-iteration. These results demonstrate that global optimality is important in designing nonconservative controllers. Computational results demonstrate that the algorithm is capable of designing globally optimal robust controllers for processes of moderate dimension.

Acknowledgements

The first author was supported by the UIUC Computational Science and Engineering Program. The second author was supported by the DuPont Young Faculty Award. The third author was supported by the Petroleum Research Fund and the National Science Foundation under grant DMII94-14615.

References

[1] M. Morari, E. Zafiriou., Robust Process Control, Prentice Hall, Englewood Cliffs, NJ, 1989.
[2] S. Skogestad, I. Postlethwaite, Multivariable Feedback Control: Analysis and Design, Wiley, New York, 1996.
[3] M.A. Rotea, T. Iwasaki, An alternative to the D-K iteration?, in: Proc. of the American Control Conf., IEEE Press, Piscataway, NJ, 1994, pp. 53–57.
[4] K.-C. Goh, M.G. Safonov, G.P. Papvassilopoulos, A global optimization approach for the BMI problem, in: Proc. of the IEEE Conf. on Decision and Control, IEEE Press, Piscataway, NJ, 1994, pp. 2009–2014.
[5] Y. Yamada, S. Hara, H. Fujioka, Global optimization for constantly scaled H_∞ control problem. in: Proc. of the American Control Conf., IEEE Press, Piscataway, NJ, 1995, pp. 427–430.
[6] S. Boyd, L. El Ghaoui, E. Feron, V. Balakrishnan, Linear Matrix Inequalities in System and Control Theory, vol. 15 of Studies in Applied Mathematics, SIAM, Philadelphia, PA, 1994.
[7] P. Gahinet, A. Nemirovskii, LMI Lab: a package for manipulating and solving LMIs, 1993, (computer software).
[8] S. Boyd, S. Wu, sdpsol: a Parser/Solver for Semidefinite Programs with Matrix Structure, Stanford University, Stanford, CA, 1996.

[9] J.S. Shamma, Necessity of the small-gain theorem for time-varying and nonlinear systems, IEEE Trans. on Auto. Control 36, (1991) 1138–1147.
[10] J.S. Shamma, Robust stability analysis of time-varying systems using time-varying quadratic forms, Syst. and Control Let. 24, (1995) 13–17.
[11] K. Zhou, J.C. Doyle, K. Glover, Robust and Optimal Control, Prentice Hall, Englewood Cliffs, NJ, 1995.
[12] H.S. Ryoo, N.V. Sahinidis, Global optimization of nonconvex NLPs and MINLPs with applications in process design, Comp. & Chem. Eng. 19, (1995) 551–566.
[13] H.S. Ryoo, N.V. Sahinidis, A branch-and-reduce approach to global optimization, J. of Global Optimization 8, (1996) 107–139.
[14] G.P. McCormick, Nonlinear Programming. Theory, Algorithms, and Applications, Wiley Interscience, New York, 1983.
[15] Y. Yamada, S. Hara, H. Fujioka, H_∞ control problem with constant diagonal scaling—global optimization for output feedback case, in: Proc. SICE Symp. on Dynamical Systems Theory, November 1994, pp. 77–82.
[16] B. Wie, D.S. Bernstein, Benchmark problems for robust control design, in: Proc. of the American Control Conf., IEEE Press, Piscataway, NJ, 1990, pp. 961–962.
[17] J.G. VanAntwerp, R.D. Braatz, N.V. Sahinidis, Globally optimal robust control of large scale sheet and film processes, in: Proc. of the American Control Conf., IEEE Press, Piscataway, NJ, 1997, pp. 1473–1477.
[18] D.G. Ballegeer, Selective reactive ion etching in silicon tetrachloride/silicon tetraflouride plasmas for gate recess in gallium arsenide-based MODFET fabrication, M.S. thesis, University of Illinois, Urbana, IL, 1992.
[19] B.A. Rashap, M.E. Elta, H. Etemad, J.P. Fournier, J.S. Giles, M.D. Giles, J.W. Grizzle, P.T. Kabamba, P.P. Khargonekar, S. Khargonekar, J.R. Moyne, D. Teneketzis, F.L. Terry, Control of semiconductor manufacturing equipment: real-time feedback control of a reactive ion etcher, IEEE Trans. on Semiconductor Manufacturing 8, (1995) 286–297.
[20] T.L. Vincent, P.P. Khargonekar, B.A. Rashap, F. Terry, M. Elta, Nonlinear system identification and control of a reactive ion etcher, in: Proc. of the American Control Conf., IEEE Press, Piscataway, NJ, 1994, pp. 902–906.
[21] J.G. VanAntwerp, Globally optimal robust control for systems with nonlinear time-varying perturbations, M.S. thesis, University of Illinois, Urbana, IL, http://brahms.scs.uiuc.edu/~jva/thesis.pdf, 1997.
[22] T. Iwasaki, R.E. Skelton, All solutions for the general H_∞ problem: LMI existence conditions and state space formulas, Automatica 30, (1994) 1307–1317.
[23] P. Gahinet, P. Apkarian, A linear matrix inequality approach to H_∞ control, Int. J. of Robust and Nonlinear Control 4, (1994) 421–448.
[24] L. El Ghaoui, P. Gahinet, Rank minimization under LMI constraints: a framework for output feedback problems, in: Proc. of the European Control Conf., 1993, pp. 1176–1179.